

# A combined experimental and theoretical study on diglyme + 1-alkanol liquid mixtures

J.L. Trenzado<sup>a,\*</sup>, S. Rozas<sup>b</sup>, M.N. Caro<sup>a</sup>, M. Atilhan<sup>c</sup>, S. Aparicio<sup>b,\*</sup>

<sup>a</sup> Departamento de Física, Universidad de Las Palmas de Gran Canarias, 35017 Las Palmas G.C., Spain

<sup>b</sup> Department of Chemistry, University of Burgos, 09001 Burgos, Spain

<sup>c</sup> Department of Chemical Engineering and Paper Engineering, Western Michigan, Kalamazoo, MI 49008-5462, USA

## ARTICLE INFO

### Article history:

Received 27 November 2020

Revised 5 March 2021

Accepted 31 March 2021

Available online 6 April 2021

### Keywords:

Liquid mixtures

Glymes

Alcohols

Hydrogen bonding

Thermophysics

Molecular simulation

## ABSTRACT

The properties, structuring and intermolecular forces of diglyme + alkanol mixtures are studied using a combined experimental and theoretical approach. The thermophysical properties as well as the molecular simulation results provide detailed characterization of the mixtures in terms of composition, type of 1-alkanol and temperature. The possibility of development of heteroassociations by glyme - alkanol hydrogen bonding as well as their effect on the weakening and breaking on alkanols self-association show a pivotal role on the mixtures structure as well as the glyme self-association. The reported mixtures show complex structural effects varying with mixtures composition which may be considered as model of ether - hydroxyl interaction and their effects on the mixture's properties and nature.

© 2021 Elsevier B.V. All rights reserved.

## 1. Introduction

The knowledge of complex liquid mixtures behavior (intermolecular forces or hydrogen bonding effect) is of special both practical and theoretical interest for several purposes [1,2]. Mixed fluids require a precise combination of macroscopic properties study, based on the nature and extension of the intermolecular interactions, and nanoscopic level characterization for the accurate hydrogen bonding analysis [3]. Additionally, thermophysical properties are of relevant importance for process design [4] development from an economic and operational performing operations point of view [4,5]. There is a huge amount of combined solvents which are being considered for industrial processes, for this reason a precise selection and a systematic approach is required to optimize physicochemical properties of complex mixed fluids for industrial purposes. Intermolecular interactions are usually analyzed in complex fluids through physicochemical properties as a function of the composition evolution, pressure or temperature. It is important to consider both microscopic structures and intermolecular interactions. Likewise, macroscopic physicochemical properties of the complex mixed liquids contribute to the under-

standing of hydrogen bonding properties and features. The effect of chemical composition in terms of mole ratios is also largely relevant. Therefore, the relationships between all these factors should be considered. In terms of complex mixed liquids, the consideration of applicable functional groups and molecules, evaluating the main characteristics of the intermolecular forces developed among them is a suitable approach to systematize the study of such fluids of interest. In the recent years special attention has been paid to pairs of functionalized organic molecules, where one of the molecules act as hydrogen donor (H-donor) while the other as hydrogen acceptor (H-acceptor). The case of alcohols is considered of special relevance as the presence of the hydroxyl group [6] may give alcohol molecules both roles [7] (H-donor and H-acceptor), in addition to the inclusion of non-polar groups leading to hydrogen bonding formation [32], generally depending on the chain extension and location of the hydroxyl group. Nonetheless, different type of molecules, such as glymes [8], amides [9], ethers [10], ionic liquids [11] or deep eutectic solvents [12] have also been studied by our group, combining experimental and theoretical approaches in order to report hydrogen bonding behavior. With the purpose of carrying on the research into different binary liquid mixtures, a combined experimental and theoretical study on the properties of diethylene glycol methyl ether (diglyme, 2G) and 1-alcohols (ethanol, C2OL; 1-pentanol, C5OL; 1-octanol, C8OL), as a function of mixture composition and temperature, has been reported.

\* Corresponding authors.

E-mail addresses: [jose.trenzado@ulpgc.es](mailto:jose.trenzado@ulpgc.es) (J.L. Trenzado), [sapar@ubu.es](mailto:sapar@ubu.es) (S. Aparicio).

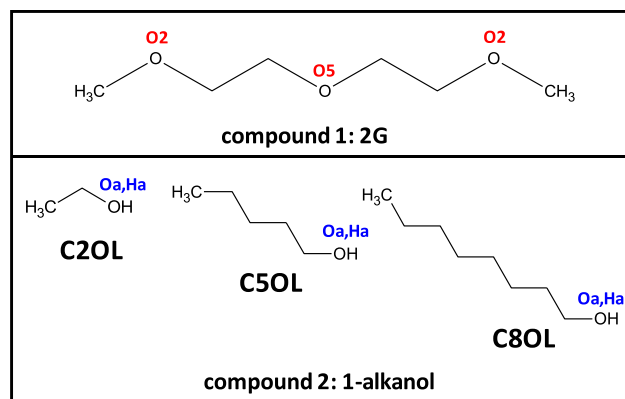


**Fig. 1.** Compounds considered in this work for compound 1 (2G) + compound 2 (1-alkanol) binary mixtures. Red and blue labels indicate atomic naming along the work.

Diglyme has been widely used recently as solvent [13] in a broad variety of applications such as sodium-ion batteries for energy storage [14–16], CO<sub>2</sub> capture absorbent solvent [17–20]; but also, as an active pharmaceutical ingredient (API) formation compound [21–23] as well as improved biodiesel [24]. Diglyme is a dipolar aprotic solvent which possess a high chemical stability, low vapor pressure and high boiling point, this is it stays liquid in a wide range of temperatures [13]. It manifests a moderate toxicity [25,26] when compared to traditional organic solvents (THF, toluene, etc.). The presence of three ether groups (easily

H-acceptor) in 2G structure has been extensively used for tuning mixture properties when it is present as a cosolvent. It has been found in the literature studies reporting the use of diglyme as solvent for CO<sub>2</sub> gas capture [27,28]. Alcohols are a commonly used family of compounds in the chemical industry, especially for applications such as biofuels [29–31]. The presence of hydroxyl groups, leading to both hydrogen donor and acceptor performance [32], gives way to complex effects scaling from hydrogen bonding changes upon mixing [33]. Therefore, it is important to note the utilization of high volatile alcohols as solvent like glymes. The aim of the present work is to study the physicochemical properties of liquid mixtures of diglyme and three different alcohols in the whole composition range.

Binary liquid mixtures of 2G + {C2OL or C5OL or C8OL}, Fig. 1, were studied in the whole composition range at macroscopic level (experimental thermophysical properties) and microscopic level (molecular modelling). Density Functional Theory (DFT) quantum chemistry method and Molecular Dynamics (MD) simulations were combined for the molecular modelling studies. The results combination from analyzed properties cited above of the binary mixtures allowed a complete (macro and microscopic) characterization, showing hydrogen bonding changes with mixture composition and temperature effects.

## 2. Methods

### 2.1. Materials

The chemicals used along this work are reported in Table S1 (Supplementary Information). They were used as received from

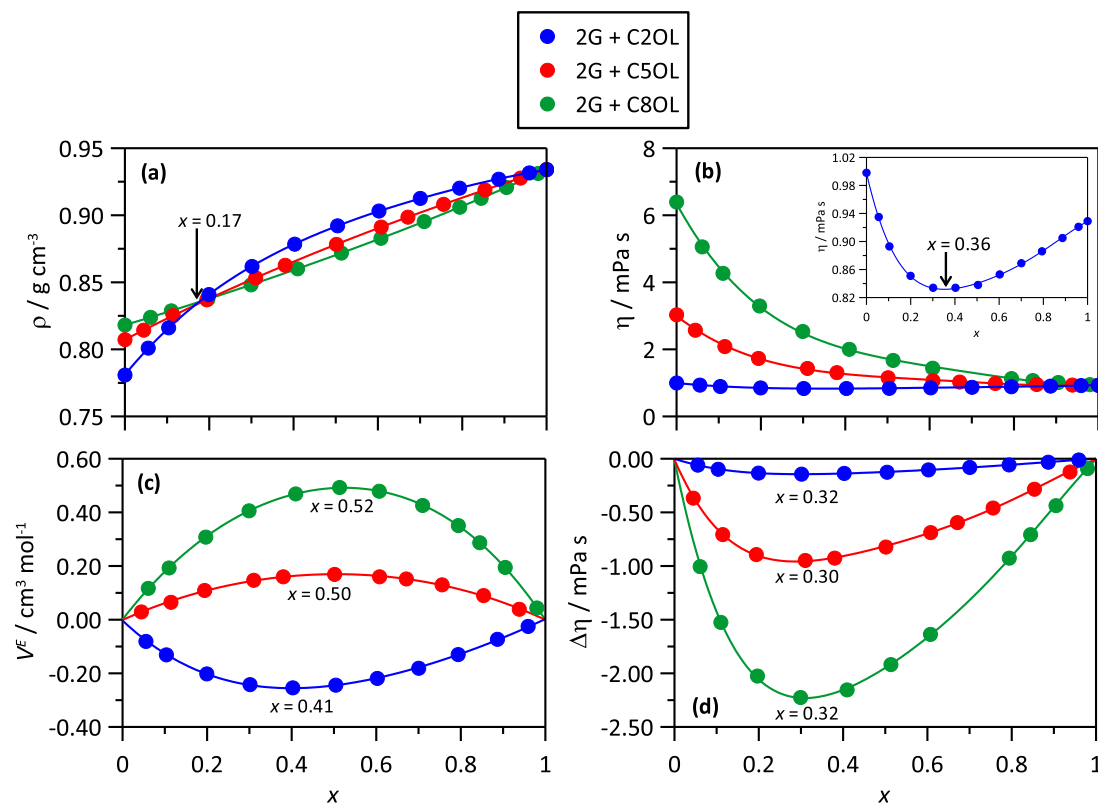


**Fig. 2.** (a) Experimental density,  $\rho$ , (b) dynamic viscosity,  $\eta$ , (c) excess volume,  $V^E$ , and (d) mixing viscosity,  $\Delta\eta$ , for  $\times 2G + (1-x)$  {C2OL or C5OL or C8OL},  $x$  stands for mole fraction, at 303.15 K and 0.1 MPa. Circles stand for experimental data and lines for polynomial ( $\rho$  and  $\eta$ ) or Redlich-Kister ( $V^E$  and  $\Delta\eta$ ) fits.

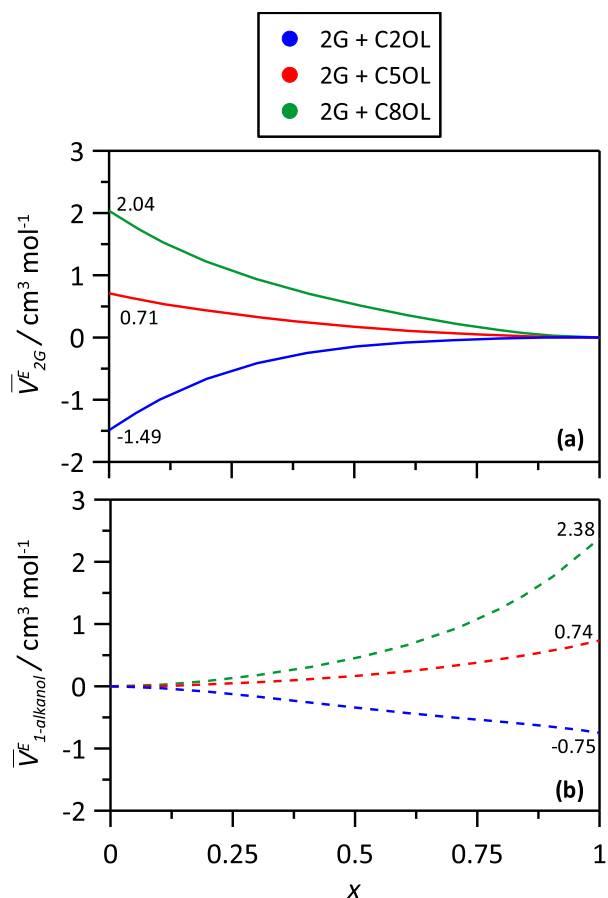


**Fig. 3.** Excess partial volume,  $\bar{V}_i^E$ , of  $i$  component, (a) for  $i = 2G$  and (b)  $i = 1$ -alkanol, in  $x \times 2G + (1 - x) \{C2OL \text{ or } C5OL \text{ or } C8OL\}$ ,  $x$  stands for mole fraction, at 303.15 K and 0.1 MPa. Values inside the panels show infinite dilution data,  $\bar{V}_i^{E,\infty}$ .

the commercial supplier without further purification and kept under molecular sieves (4 nm, Union carbide) before mixtures preparation. Density and viscosity were experimentally determined in the 283.15–313.15 K range for pure fluids and compared with available literature information, thus showing excellent agreement, which is considered as validation for the purity of the chemicals and the experimental procedures applied along this work. Binary mixtures were prepared by weighing with a Mettler

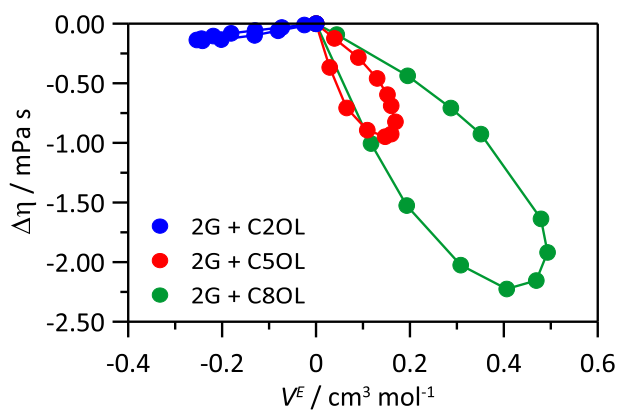


**Fig. 4.** Relationship between excess molar volume,  $V^E$ , and mixing viscosity,  $\Delta\eta$ , for  $x \times 2G + (1 - x) \{C2OL \text{ or } C5OL \text{ or } C8OL\}$ ,  $x$  stands for mole fraction, at 303.15 K and 0.1 MPa.

AE240 balance ( $\pm 0.01$  mg) thus leading to mole fraction uncertainty of  $\pm 0.00005$ .

## 2.2. Thermophysical properties

The density ( $\rho$ ) and dynamic viscosity ( $\eta$ ) of the pure solvents and binary mixtures were measured in the 283.15–313.15 K range, at atmospheric pressure conditions. Density data were collected using a vibrating tube densimeter (Anton Paar DMA61/602), calibrated with water (Panreac Hiperpur-plus) and n-heptane (Fluka > 99.5%) as reference fluids [34,35], with the cell temperature measured to  $\pm 0.01$  K uncertainty, thus leading to  $\pm 0.00002$  g  $\times$  cm $^{-3}$  uncertainty. Capillary viscometer (Schott-Geräte AVS350) was used for measuring the kinematic viscosity ( $\nu$ ), calibrated with standard reference oils, and the cell temperature measured to  $\pm 0.01$  K uncertainty, therefore leading to 0.4% uncertainty in viscosity. Dynamic viscosity was calculated from kinematic viscosity and density data.

Several derived thermodynamic properties were calculated from experimental  $\rho$  and  $\eta$  data (Supplementary Information, Table S5): i) Isobaric expansivity,  $\alpha_p$ , and excess isothermal compressibility,  $\alpha_p^E$ , ii) excess molar volume,  $V^E$ , iii) partial molar volumes of each  $i$  compound in a mixture,  $\bar{V}_i$ , the corresponding excess value,  $\bar{V}_i^E$ , and the value at infinite dilution,  $\bar{V}_i^{E,\infty}$ . For the dynamic viscosity, the so-called mixing viscosity,  $\Delta\eta$  was calculated.

## 2.3. Molecular modelling

Dimers' interactions were studied carrying out DFT molecular modelling using ORCA program [36] with B3LYP [37–39] functional, 6-311++G(d,p) basis set and D3 [40] dispersion contribution (semiempirical Grimme's method). Monomers and dimers 2G + {2COL, 5COL or C8OL} 1:1 were optimized considering the different hydrogen bonding sites at 2G. Interaction energies,  $\Delta E$ , were calculated as the difference between the dimer energy and the sum of the corresponding monomers energy corrected according to counterpoise method [41]. Calculation of vibrational spectra for the optimized geometries probed the obtention of global minima, allowing to discard negative frequencies. Topology of hydrogen bonding was analyzed using Bader's Atoms in a Molecule (AIM [42]) theory using MultiWFN software [43].

MD simulations were carried out with MDynaMix v.5.2 [44] software, using the force field parametrizations described in Table S3 (Supplementary information). SwissParam database was used to obtain force field parameters derived from the Merck Molecular Force Field [45]. Systems analyzed through MD simulations of 2G + alcohol mixtures are reported in Table S4 (Supplementary Information) and were designed to analyze the binary mixtures in the full composition range using 500 total molecules. Initial cubic simulation boxes were built with Packmol [46] program with low densities for the systems (1 g cm $^{-3}$  for all mixtures). Simulations were performed in two steps starting with 10 ns NVT optimization at 503 K (examined by the evolution of the total potential energy), followed by NPT runs (50 ns long) at 303 K and 1 bar. Nose-Hoover method was used to manage pressure and temperature. Tuckerman-Berne double time step (1 and 0.1 fs for long and short-time steps) algorithm was applied for the equations of motion [47]. Electrostatic interactions were treated with Ewald method (15 Å for cut-off radius) [48] and Lennard-Jones interactions (15 Å for cut-off) were calculated considering Lorentz-Berthelot mixing rules. MD simulations were analyzed using TRAVIS software [49] to obtain insights into the structure and dynamics of intermolecular forces.

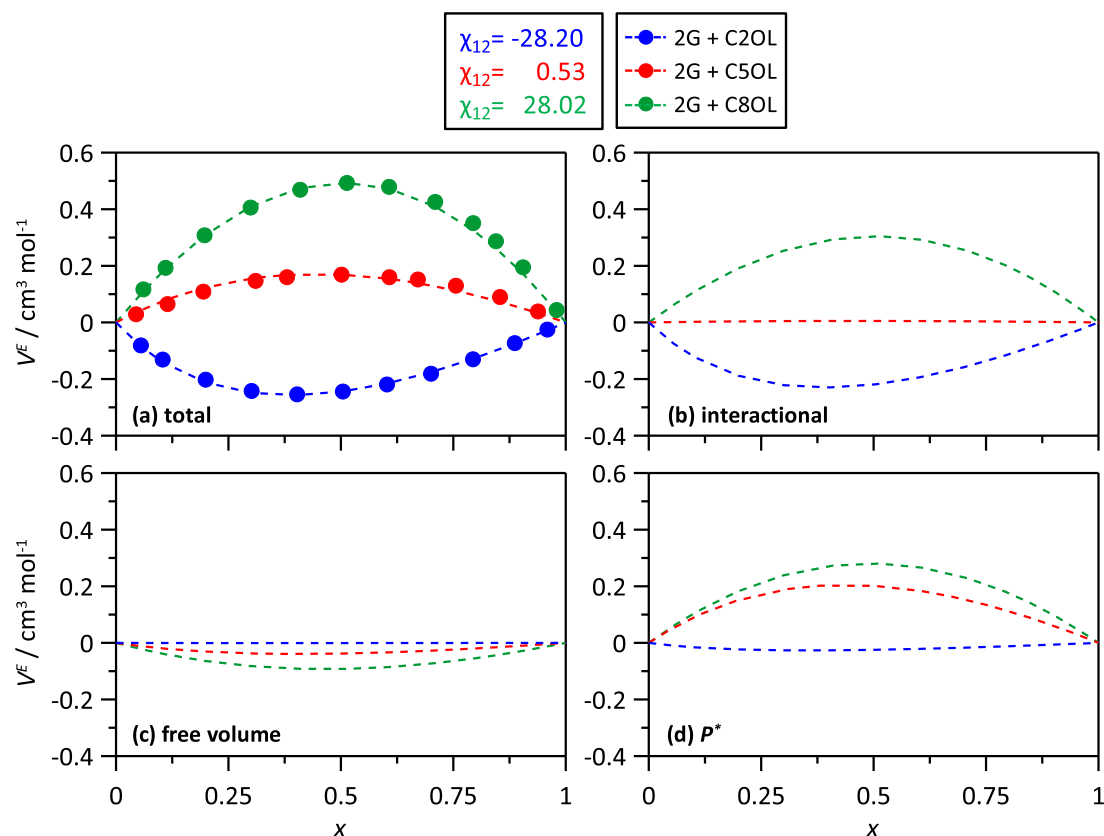


**Fig. 5.** (a) Comparison of experimental, exp, and Prigogine-Flory-Patterson, PFP, excess molar volume,  $V^E$ , for  $\times$  2G + (1 -  $\times$ ) {C2OL or C5OL or C8OL},  $\times$  stands for mole fraction, at 303.15 K and 0.1 MPa.  $\chi_{12}$  stands for PFP interaction parameter. Results show (b) interactional, (c) free volume and (d)  $P^*$  PFP contributions to the total  $V^E$ . Optimized  $\chi_{12}$  parameters used for calculations are also reported.

### 3. Results and discussion

#### 3.1. Experimental study

Experimental thermophysical properties of 2G + 1-alkanol (ethanol, 1-pentanol and 1-octanol) are reported in Tables S5 to S10 (Supplementary Information). Likewise,  $V^E$  and  $\Delta\eta$  in the 283.15 to 313.15 K temperature range are in Figs. S1 to S6 (Supplementary Information). Experimental density data are reported in Fig. 2a showing a largely non-linear (non-ideal) behavior for the three studied 1-alkanols. For  $\times$  (2G mole fraction) lower than 0.17 the density ordering is C8OL mixtures > C5OL mixtures > C2OL mixtures whereas for  $\times$  > 0.17 the ordering is reversed C8OL mixtures > C5OL mixtures > C2OL mixtures. Therefore, for 1-alkanol rich mixtures the structuring seems dominated by the trend of the 1-alkanol to self-associate, both through hydrogen bonding and stacking of alkyl chains, which leads to larger densities for the larger alkanols, whereas as the 2G content increases the shorter alkanols led to larger densities, which may be justified considering that smaller alkanols are able to fit more properly into the mixtures structure dominated by the trend of 2G molecules to self-associate as well as for the larger disrupting effect of 2G on the self-interaction of 1-alkanols. In the case of viscosity, Fig. 2b, a largely non-linear behavior is inferred, with larger deviations from linear evolution as the 1-alkanol chain increases considering their larger viscosities. In the case of ethanol containing mixtures, a minimum in viscosity is inferred at  $\times = 0.5$ . For C5OL and C8OL mixtures the non-linear behavior of viscosity shows three composition regions. The first one up to  $\times = 0.3$ , with a sharp decrease of viscosity, which raises from the disrupting effect of 2G on alkanol

self-hydrogen bonding. The second one in the  $\times = 0.3$  to 0.7, with a weaker decrease of viscosity, which would correspond to a transitional region between mixtures dominated by the alkanols and those dominated by the 2G. The third one for  $\times > 0.7$ , with minor changes in viscosity, corresponding to mixtures dominated by 2G structuring. The values of  $V^E$  reported in Fig. 2c, show negative values for C2OL mixtures and positive ones for C5OL and C8OL mixtures. The densification upon mixing for C2OL mixtures led to negative  $V^E$  values with minima at roughly  $\times = 0.4$  whereas for C5OL and C8OL maxima at roughly  $\times = 0.5$  are inferred. Therefore, perturbative effects upon mixing, i.e. larger values of  $V^E$  are inferred for close to equimolar mixtures. This effect appears both for contraction and expansion effects, thus indicating that the behavior of the mixtures is characterized by a dilution effect of each type of intermolecular forces more than from the development of strong heteroassociations. Likewise, the relevance of steric effects rising from the size of the alkanol in comparison with the 2G is a relevant factor. In the case of  $\Delta\eta$ , Fig. 2d, negative values are inferred for the three studied 1-alkanols, increasing (in absolute value) in the ordering C2OL < C5OL < C8OL, which corresponds to larger perturbative effect by 2G on the alkanol self-interactions when the alkanol chain increases. The minima of  $\Delta\eta$  curves appear at  $\times = 0.30$ , which show the larger disruptive effect for alkanol rich mixtures, i.e. 2G mixtures weaken alkanol self-interactions, decreasing viscosity, both through hindering alkanol hydrogen bonding and interaction between alkyl chains. The packing effects are also inferred from the excess partial molar volumes,  $\bar{V}_i^E$ , for 2G and 1-alkanol, Fig. 3. In agreement with the sign of  $V^E$ ,  $\bar{V}_i^E$  is negative for C2OL and positive for C5OL and C8OL mixtures. Values at

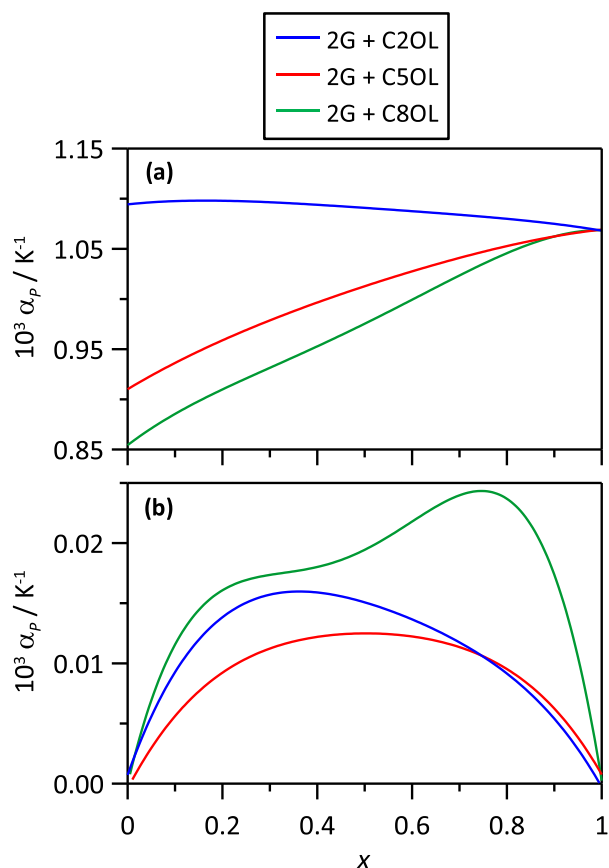


**Fig. 6.** (a) Isobaric expansivity,  $\alpha_p$ , and (b) excess isobaric expansivity,  $\alpha_p^E$ , in for  $x \times 2\text{G} + (1-x) \{\text{C2OL or C5OL or C8OL}\}$ ,  $x$  stands for mole fraction, at 303.15 K and 0.1 MPa.

infinite dilution (when  $x$  or  $1-x \rightarrow 0$ ) being negative for C2OL in 2G and also for 2G in C2OL confirm that short alkanol molecules are able to fit into the 2G structuring, and vice versa, whereas the positive values for C5OL and C8OL confirm the disruptive effect of these alkanols on 2G liquid structuring and vice versa. The completely different behavior of C2OL mixtures in comparison with C5OL and C8OL ones is confirmed by the  $V^E$  vs  $\Delta\eta$  plots reported in Fig. 4, the size of the lobular curves increases on going from C2OL to C5OL to C8OL, thus the non-ideality of the mixtures as well as the completely different behavior of mixtures with short alkanols in comparison with large ones.

The experimental  $V^E$  was analyzed using the Prigogine-Flory-Patterson (PFP) model, to infer and split the main contributions to this relevant property. The parameters required for the application of PFP model are reported in Table S11 (Supplementary Information). The PFP model is able to describe  $V^E$  with a single fitting parameter ( $\chi_{12}$ ), Fig. 5a. The PFP model considers three different contributions to the total  $V^E$ : interactional, free volume and  $P^*$ , which accounts the difference of internal pressure and reduced volume of components. The interactional contribution, which is dependent on  $\chi_{12}$ , considers intermolecular interactions (although not explicitly defining hydrogen bonding) being negative for C2OL, almost null for C5OL and positive for C8OL, which agrees with the values and sign of  $\chi_{12}$  parameters, Fig. 5b. The free volume contributions, Fig. 5c, are lower than the other two ones and show packing effects increasing with the increasing size of the 1-alkanol. Regarding the characteristic pressure contributions, Fig. 5d, they are large and follow the same trend that the interactional contribution, being negative for C2OL and positive for C5OL and C8OL,

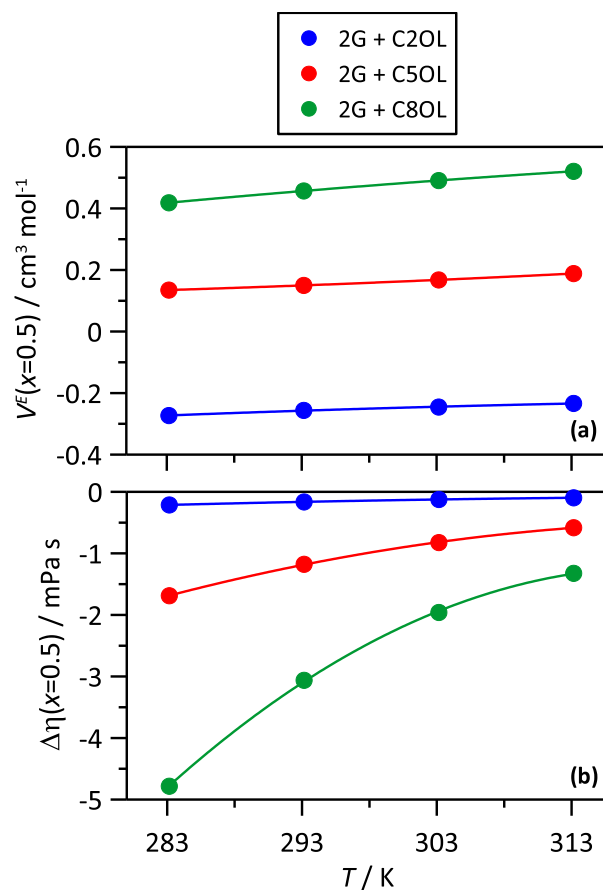


**Fig. 7.** Temperature effect on the value of (a) excess molar volume and (b) mixing viscosity at equimolar composition,  $V^E(x=0.5)$  and  $\Delta\eta(x=0.5)$ , for  $x \times 2\text{G} + (1-x) \{\text{C2OL or C5OL or C8OL}\}$ .

showing the structure breaking effects for the longer alkanols. Therefore, from the PFP analysis it may be inferred that intermolecular interactions decrease upon increasing alkanol size as well as the structure breaking effect, which are the origin of  $V^E$  behavior.

The  $\alpha_p$  and  $\alpha_p^E$  are reported in Fig. 6. In the case of  $\alpha_p$ , the values for C2OL mixtures are larger than for C5OL and C8OL mixtures, i.e. C2OL mixtures are more expansible than those with the larger alkanols, which may be related with the sign of  $V^E$  and the contributions inferred from PFP model. Nevertheless,  $\alpha_p^E$  values in Fig. 6b are positive for the three studied alkanols, and although the values are small show that mixing with 2G leads to an increase in the expansibility, which may be related with the weakening of intermolecular forces and the structure breaking effects upon mixing.

The temperature effect on  $V^E$  and  $\Delta\eta$  are reported in Fig. 7. For the case of  $V^E$ , values follow a linear evolution with temperature, decreasing (in absolute value) for C2OL and increasing (as positive) for C5OL and C8OL, i.e. the increasing temperature increases the positive, expansive, contributions to the total  $V^E$ , mainly by weakening of intermolecular interactions and increasing the structure breaking effects. In the case of  $\Delta\eta$ , Fig. 7b, non-linear evolution with temperature is inferred, especially for the longer alkanols, decreasing (in absolute value) with increasing temperature. The effect of temperature on  $\Delta\eta$  is larger than on  $V^E$ , which may justify with the weakening of intermolecular forces in pure solvents, thus leading to lower effects upon mixing, i.e. the disrupting effect of the presence of 2G on alkanols self-hydrogen effect decreases upon heating. The activation energy from viscosity data,  $E_a$ , was

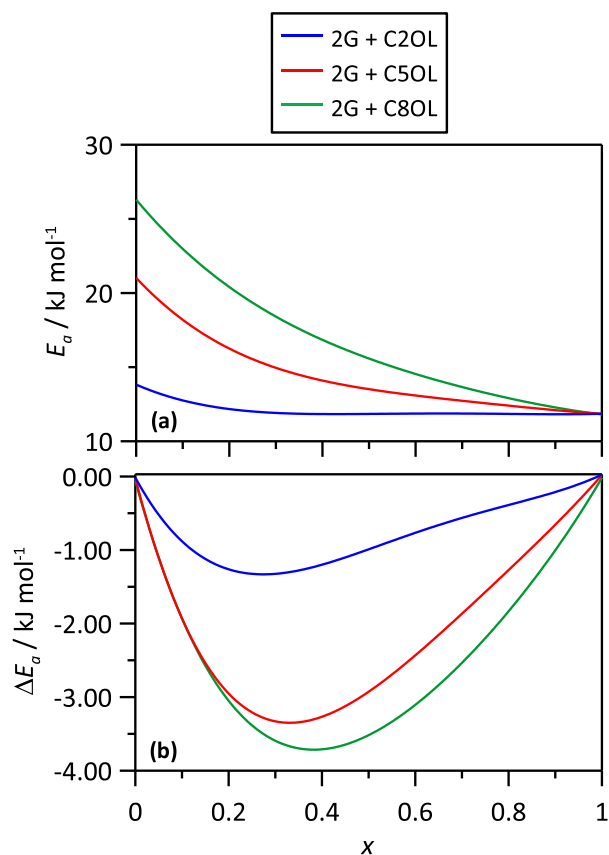


**Fig. 8.** (a) Activation energy,  $E_a$ , and (b) deviations from linearity of  $E_a$ ,  $\Delta E_a$ , from the fit of experimental dynamic viscosity as a function of temperature to Arrhenius equation in for  $x \times 2G + (1 - x)$  {C2OL or C5OL or C8OL},  $x$  stands for mole fraction, at 0.1 MPa.

calculated from Arrhenius equation and reported in Fig. 8a. The  $E_a$  values follow the C2OL < C5OL < C8OL ordering, in agreement with increasing viscosity for the increase of alkanol chain length. The evolution of  $E_a$  with 2G content follows a non-linear evolution, thus leading to 2G – rich mixtures with  $E_a$  values almost indepen-

dent of the type of alkanol, i.e. similar disrupting effect of 2G for low alkanol content, whereas for alkanol – rich mixtures the values are largely dependent on the type of alkanol. The deviations from linearity of  $E_a$ ,  $\Delta E_a$ , are negative for all the considered mixtures, Fig. 8b, thus confirming the structure breaking effect of 2G on the alkanol structuring. Additional information on the temperature effect on the studied mixtures can be inferred from the evolution of  $\bar{V}_i^{E,\infty}$ , for all the cases showing a linear decrease (in absolute value) with increasing temperature, Fig. 9. The negative values of  $\bar{V}_i^{E,\infty}$  for 2G in C2OL, Fig. 9a, are maintained in the studied temperature range, showing that the minor disruptive effect of C2OL is only slightly increased upon heating, and analogously for C2OL in 2G, Fig. 9b. For C5OL and C8OL, the positive  $\bar{V}_i^{E,\infty}$  increasing upon heating show the reinforcement of the disruptive effect of 2G on alkanol and vice versa, i.e. further weakening of intermolecular forces and increase of structure breaking effects.

### 3.2. Molecular modelling

The nanoscopic properties of the studied mixtures were also studied using molecular simulation results with particular attention to intermolecular forces. In a first approach, DFT studies were carried out for 2G : alkanol dimers to infer the nature of the possible heteroassociations by hydrogen bonding. The 2G – alkanol hydrogen bonds were analyzed considering all the possible 2G acceptor sites, i.e. terminal and central oxygen atoms in the 2G molecules, Fig. 10. The calculated  $\Delta E$  values are independent of the interaction site in the 2G molecule as well as of the type of 1-alkanol, with values in the  $-49.1$  to  $-49.8 \text{ kJ mol}^{-1}$  range. These values confirm the possible development of strong 2G to 1-alkanol heteroassociation through hydrogen bonding as inferred from  $\Delta E$ , hydrogen to oxygen distance (roughly  $1.9 \text{ \AA}$  for all the cases) and from the AIM topological analysis. Binary critical points, BCPs, appear for all the possible hydrogen bonding sites, with the values of the electron density,  $\rho$  ( $\approx 0.03$ ), and the corresponding laplacians,  $\nabla^2 \rho$  ( $\approx 0.11$ ), at these BCPs in the upper limit of the values commonly used to define strong hydrogen bond: i)  $0.002$ – $0.014$  a.u. for  $\rho$  and ii)  $0.014$ – $0.139$  a.u. for  $\nabla^2 \rho$  with stronger interactions for larger values [50].

Therefore, the possibility of developing 2G – alkanol strong hydrogen bonding is confirmed through DFT results; nevertheless,

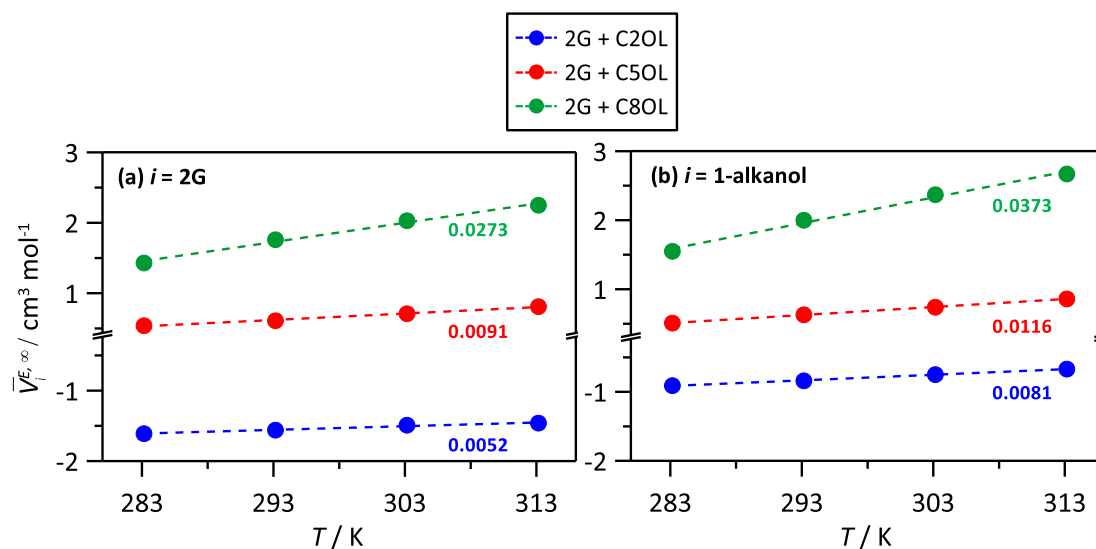


**Fig. 9.** Excess partial molar volume at infinite dilution,  $\bar{V}_i^{E,\infty}$ , of  $i$  component, (a) for  $i = 2G$  and (b)  $i = 1\text{-alkanol}$ , in  $x \times 2G + (1 - x)$  {C2OL or C5OL or C8OL},  $x$  stands for mole fraction, as a function of temperature and 0.1 MPa. Values inside the panels close to each line indicate values of the slope  $\frac{d\bar{V}_i^{E,\infty}}{dT}$ .

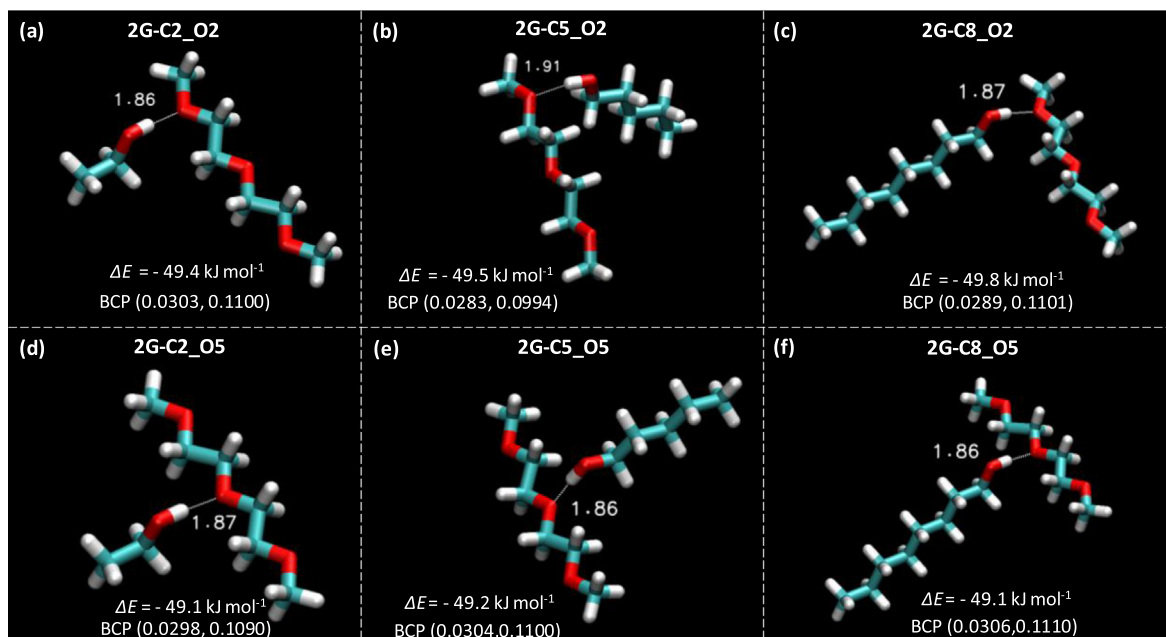


**Fig. 10.** DFT optimized structures for 1 (2G) : 1 (1-alkanol) dimers indicating counterpoise corrected binding energies,  $\Delta E$ , H (OH in 1-alkanol) – O (2G) distance (in Å), and results of AIM analysis for the BCPs in the bond path joining H (OH in 1-alkanol) – O (2G) reporting BCP( $\rho, \nabla^2\rho$ ) in a.u., where  $\rho$  and  $\nabla^2\rho$  stands for the electronic density and the corresponding Laplacian at BCP.

in the liquid state it should be considered the competing effects rising from the presence of larger molecular clusters, the competing effect of alkanols strong self-association through hydrogen bonds as well as steric effects. These effects were analyzed using MD simulations of the studied mixtures as a function of composition. The number of hydrogen bonds per 1-alkanol molecule,  $N_{H-bonds}$ , both for heteroassociations (2G – alkanol, Fig. 11a) and homoassociations (alkanol – alkanol, Fig. 11b) were calculated from MD simulations. Results for 2G – alkanol hydrogen bonding, Fig. 11a, show that in spite of the DFT results confirming the possibility of developing this type of hydrogen bonding, it is only present for 2G – rich mixtures. The extension of heteroassociation, although slightly increasing with the size of the alkanol follows the same for all of them. The alkanol self-association, Fig. 11b, is maintained up to close to equimolar mixtures and then it starts to decrease by the formation of heteroassociations with 2G molecules. The composition evolution of  $N_{H-bonds}$  follows a non-linear trend, in parallel to the behavior of experimental properties reported in previous sections. For the mixtures up to  $x = 0.5$ , the alkanol self-association shows minor disruption by the presence of 2G molecules. In the case of the 0.5–0.7 mol fraction range, alkanol self-hydrogen bonding starts to be disrupted in a larger extension. Finally for 2G rich mixtures ( $x > 0.7$ ) the trend of alkanols to interact with 2G molecules is the prevailing effect accompanied by the decrease of alkanols self-association. Therefore, although 2G molecules are prone to be hydrogen bonded with alkanol molecules, this trend is only relevant for 2G rich mixtures, whereas for alkanol – rich ones, the strength of alkanol hydrogen bonds as well as the extension of alkanols self-association hinders the development of hydrogen bonds with 2G.

Radial distribution functions, RDFs, were considered to analyze the molecular arrangements around each type of molecule. Results in terms of RDFs are only reported for C2OL containing systems, but analogous results were inferred for C5OL and C8OL containing mixtures. The 2G – C2OL interactions are analyzed in Fig. 12a, a first peak at 2.1 Å (slightly larger than the 1.9 Å from DFT in

Fig. 10) indicates the 2G – C2OL hydrogen bonding, although the intensity of this peak is very weak for alkanol – rich mixtures but increases with increasing 2G content, which agrees with the extension of hydrogen bonding reported in Fig. 11. The C2OL – C2OL self – association is analyzed in Fig. 12b, with the first peak

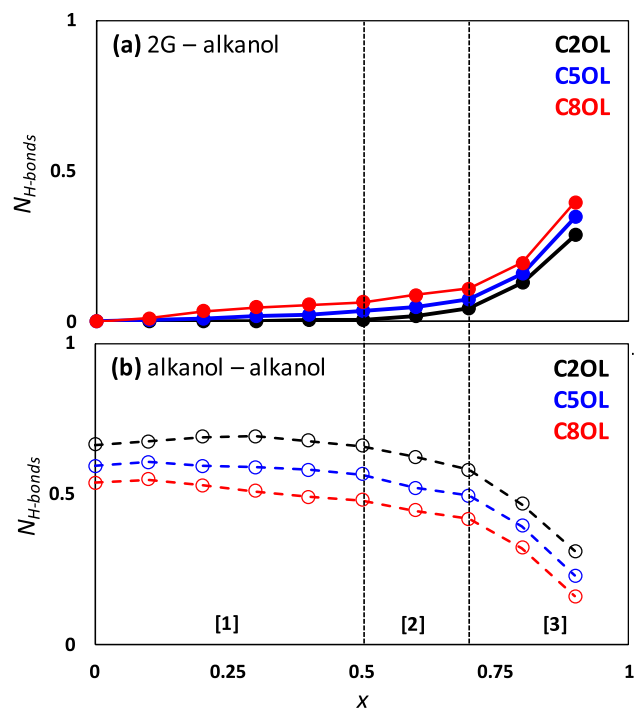


**Fig. 11.** Average number of hydrogen bonds,  $N_{H-bonds}$ , per alkanol molecule in  $x$  2G +  $(1-x)$  (C2OL or C5OL or C8OL), from MD simulations at 303 K and 0.1 MPa. Results in (a) show 2G – 1-alkanol and in (b) 1-alkanol – 1-alkanol hydrogen bonds. Hydrogen bonding criteria: 3.5 Å and 60° for donor – acceptor separation and angle. Vertical dotted lines indicate composition regions with different behaviour.

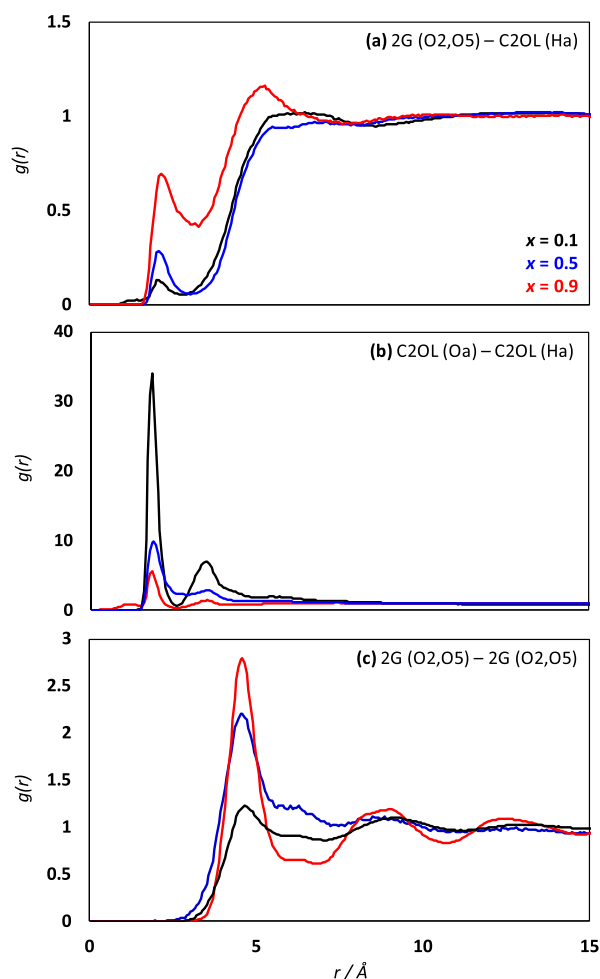


**Fig. 12.** Site – site radial distribution functions,  $g(r)$ , in  $\times 2G + (1 - x) C2OL$ , from MD simulations at 303 K and 0.1 MPa. Atom labelling as in Fig. 1. Results for (a) 2G – C2OL, (b) C2OL – C2OL and (c) 2G – 2G interactions.

at  $1.8 \text{\AA}$  confirming C2OL – C2OL hydrogen bonding but decreasing with increasing 2G content. For the possible homoassociation of 2G molecules, the intense and wide peak at  $4.5 \text{\AA}$  reported in Fig. 12c, shows that 2G molecules are largely self-associated, even for low 2G content ( $x = 0.1$ ) the presence of the RDF peak confirms this trend, which will be the reason for the low perturbative effect on C2OL self-association at low 2G content and being increased with increasing 2G content. The integration of RDFs for the first solvation shells, i.e. the first minima in Fig. 12, provides the solvation

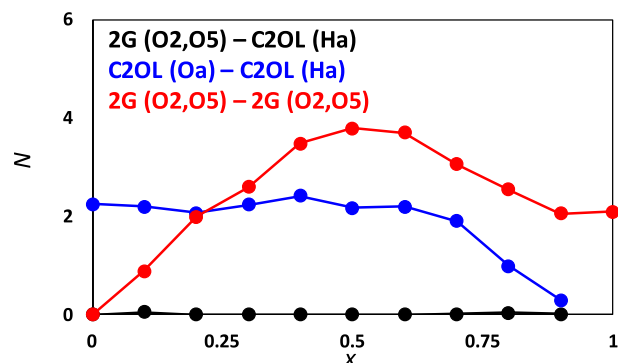


**Fig. 13.** Number of molecules around a central one,  $N$ , in the first solvation shell as defined from the first minima in the corresponding radial distribution functions (Fig. 12) in  $\times 2G + (1 - x) C2OL$ , from MD simulations at 303 K and 0.1 MPa.

numbers,  $N$ , as reported in Fig. 13. These results confirm the prevailing role of 2G self-association for 2G – rich mixtures as well as the prevailing presence of C2OL self-hydrogen bonding for  $x < 0.5$ , with these two effects, and their non-linear evolution with composition as the main factors determining the properties of the studied mixtures. From the viewpoint of interaction energies from MD,  $E_{inter}$  (Fig. 14), the 2G self-association leads to large  $E_{inter}$  values, increasing with alkanol chain length present in the mixtures. The strength of alkanol – alkanol self-interactions are maintained in the whole composition range and for 2G – alkanol interactions, although present in minor extension, Fig. 14, they are also strong in agreement with DFT results. Therefore, MD results allow to infer that the properties of these mixtures are characterized by a competing effect of alkanols and 2G self-association, i.e. showing certain degree of nanoscopic heterogeneity, whereas in spite of the possibility of developing heteroassociations, these are only relevant for 2G rich mixtures. The non-linear evolution with composition of these effects would be on the roots of the behavior of the thermophysical properties and the deviations from ideality.

#### 4. Conclusions

The properties of diglyme + 1-alkanol liquid mixtures were studied as a function of composition and temperature, using a combined experimental and molecular simulation approach. The thermophysical properties showed largely non-ideal mixtures with a strong effect from the length of alkanol chain. Mixtures with ethanol show contraction upon mixing, whereas for long alkanols such as 1-pentanol expansion is inferred. The properties and

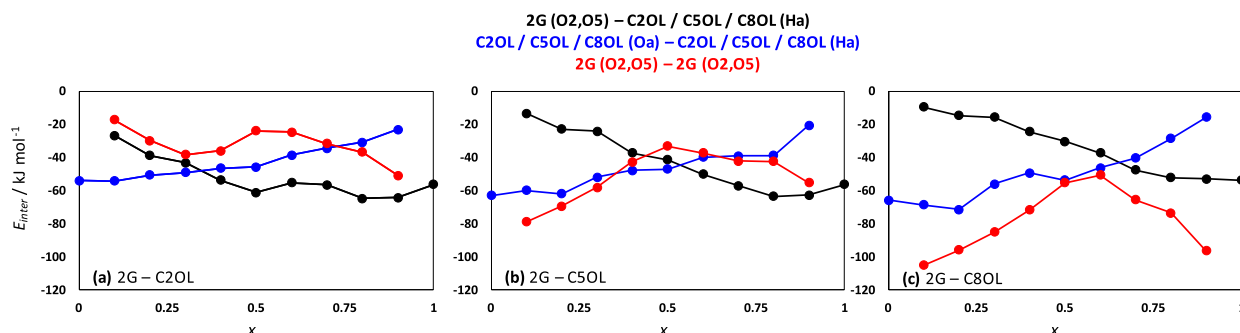


**Fig. 14.** Intermolecular interaction energy,  $E_{inter}$ , for  $\times 2G + (1 - x) [C2OL \text{ or } C5OL \text{ or } C8OL]$ , from MD simulations at 303 K and 0.1 MPa. Results for (a) 2G – C2OL, (b) 2G – C5OL and (c) 2G – C8OL mixtures.

structuring of these mixtures are characterized by the trend of both diglyme and 1-alkanol to be self-associated, with a competing effect because of the possibility of developing diglyme – alkanol heteroassociations by hydrogen bonding, although this effect and thus the weakening of alkanol hydrogen bonding is mostly relevant for diglyme rich mixtures. The properties of the mixtures may be controlled through the size of the alkanols although the nature and extension of intermolecular forces follow the same trend independently of the size of the alkanol.

### Declaration of Competing Interest

The authors declare that they have no known competing financial interests or personal relationships that could have appeared to influence the work reported in this paper.

### Acknowledgement

This work was funded Ministerio de Ciencia, Innovación y Universidades (Spain, project RTI2018-101987-B-I00). We acknowledge SCAYLE (Supercomputación Castilla y León, Spain) for providing supercomputing facilities. The statements made herein are solely the responsibility of the authors. Authors declare no competing interests.

### Appendix A. Supplementary material

Supplementary data to this article can be found online at <https://doi.org/10.1016/j.molliq.2021.116048>.

### References

- J. Gmehling, M. Kleiber, B. Kolbe, *Chemical thermodynamics for process simulation*, Ed., Wiley, Weinheim, Germany, 2019.
- M.J. Assael, The importance of thermophysical properties in optimum design and energy saving, in: Y.H. Mori, K. Ohnishi (Eds.), *Energy and Environment*, Springer, Tokio, 2001.
- N.Y. Tan, R. Li, P. Bräuer, C. D'Agostino, L.F. Gladden, J.A. Zeitler, Probing hydrogen-bonding in binary liquid mixtures with terahertz time-domain spectroscopy: a comparison of Debye and absorption analysis, *Phys. Chem. Chem. Phys.* 17 (2015) 5999–6008.
- J.M.P. Franca, C.A. Nieto de Castro, M. Matos, V. Nunes, Influence of thermophysical properties of ionic liquids in chemical process design, *J. Chem. Eng. Data* 54 (2009) 2569.
- R. Dohrn, O. Pföhl, Thermophysical properties-Industrial directions, *Fluid Ph. Equilibria*. 194–197 (2002) 15–29.
- W.O. George, B.F. Jones, R. Lewis, Water and its homologues: a comparison of hydrogen-bonding phenomena *Philos. Trans. R. Soc. London, Ser. A* 359 (2001) 1611–1629.
- K.F. Gaffney, I.R. Piletic, M.D. Fayer, Hydrogen bond breaking and reformation in alcohol oligomers following vibrational relaxation of a non-hydrogen-bond donating hydroxyl stretch, *J. Phys. Chem. A* 106 (2002) 9428–9435.
- R. Alcalde, A. Gutiérrez, M. Atilhan, J.L. Trenzado, S. Aparicio, Insights into glycol ether-alkanol mixtures from a combined experimental and theoretical approach, *J. Phys. Chem. B* 121 (2017) 5601–5612.
- R. Alcalde, G. García, J.L. Trenzado, M. Atilhan, S. Aparicio, Characterization of amide-alkanediol intermolecular interactions, *J. Phys. Chem. B* 119 (2015) 4725–4738.
- S. Aparicio, R. Alcalde, J.L. Trenzado, M.N. Caro, M. Atilhan, Study of Dimethoxyethane/Ethanol Solutions, *J. Phys. Chem. B* 115 (2011) 8864–8874.
- J.L. Trenzado, A. Gutiérrez, R. Alcalde, M. Atilhan, S. Aparicio, Insights on [BMIM][BF<sub>4</sub>] and [BMIM][PF<sub>6</sub>] ionic liquids and their binary mixtures with acetone and acetonitrile, *J. Mol. Liq.* 294 (2019) 111632.
- R. Alcalde, M. Atilhan, S. Aparicio, On the properties of (choline chloride + lactic acid) deep eutectic solvent with methanol mixtures, *J. Mol. Liq.* 272 (2018) 815–820.
- S. Tang, H. Zhao, Glymes as versatile solvents for chemical reactions and processes: from the laboratory to industry, *RSC Adv.* 4 (22) (2014) 11251–11287.
- K. Westman, R. Dugas, P. Jankowski, W. Wieczorek, G. Gachot, M. Morcrette, E. Irisarri, A. Ponrouch, M.R. Palacin, J.-M. Tarascon, P. Johansson, Diglyme based electrolytes for sodium-ion batteries, *Appl. Energy Mater.* 1 (2018) 2671–2680.
- I. Geoffroy, P. Willmann, K. Mesfar, B. Carré, D. Lemordant, Electrolytic characteristics of ethylene carbonate-diglyme-based electrolytes for lithium batteries, *Electrochim. Acta* 45 (2000) 2019–2027.
- P. Han, X. Han, J. Yao, L. Zhang, X. Cao, High energy density sodium-ion capacitors through co-intercalation mechanism in diglyme-based electrolyte system, *J. Power Sources* 297 (2015) 457–463.
- W. Huang, Y. Mi, Y. Li, D. Zheng, An aprotic polar solvent, diglyme, combined with monoethanolamine to form CO<sub>2</sub> capture material: solubility measurement, model correction, and effect evaluation, *Ind. Eng. Chem. Res* 54 (2015) 3430–3437.
- R. Vilcu, I. Găinar, G. Anăntescu, S. Perisanu, The solubility of CO<sub>2</sub>, H<sub>2</sub>, and N<sub>2</sub> in dimethylether–diethyleneglycol, *Rev. Roum. Chim.* 38 (1993) 1169.
- D. Kodama, M. Kanakubo, M. Kokubo, S. Hashimoto, H. Nanjo, M. Kato, Density, viscosity, and solubility of carbon dioxide in glymes, *Fluid Phase Equilib.* 302 (2011) 103.
- A. Henni, P. Tontiwachwuthikul, A. Chakma, Solubilities of carbon dioxide in polyethylene glycol ethers, *Can. J. Chem. Eng.* 83 (2005) 358.
- J. Verghese, C.J. Kong, D. Rivalti, E.C. Yu, R. Krack, J. Alcázar, J.B. Manley, D.T. McQuade, S. Ahmad, K. Belecki, B.F. Gupton, Increasing global access to the high-volume HIV drug nevirapine through process intensification, *Green Chem.* 19 (13) (2017) 2986–2991.
- M. Barniol-Xicota, R. Leiva, C. Escolano, S. Vázquez, Synthesis of Cinacalcet: an enantiopure active pharmaceutical ingredient (API), *Synthesis* 48 (06) (2016) 783–803.
- S. Diab, D.T. McQuade, B.F. Gupton, D.I. Gerogiorgis, Process design and optimization for the continuous manufacturing of Nevirapine, an active pharmaceutical ingredient for HIV treatment, *Org. Process Res. Dev.* 23 (2019) 320–333.
- H. Song, K.S. Quinton, Z. Peng, H. Zhao, N. Ladommatos, Effects of oxygen content of fuels on combustion and emissions of diesel engines, *Energies* 9 (28) (2016).
- R. Valentine, J. O'Neill, K.P. Lee, G.L. Kennedy Jr., Subchronic inhalation toxicity of diglyme, *Food Chem. Toxicol.* 37 (1999) 75–86.
- National Center for Biotechnology Information. PubChem Database. Diglyme, CID=8150, <https://pubchem.ncbi.nlm.nih.gov/compound/Diglyme> (accessed on Mar. 5, 2020)
- D. Kodama, M. Kanakubo, M. Kokubo, S. Hashimoto, H. Nanjo, M. Kato, Density, viscosity, and solubility of carbon dioxide in glymes, *Fluid Phase Equilibria* 302 (2011) 103–108.
- A. Henni, P. Tontiwachwuthikul, A. Chamka, Solubilities of carbon dioxide in polyethylene glycol ethers, *Can. J. Chem. Eng.* 83 (2005) 358–361.
- N. Yilmaz, E. Ileri, A. Atmanli, Performance of biodiesel/higher alcohols blends in a diesel engine, *Int. J. Energy Res.* 40 (2016) 1134–1143.
- N. Yilmaz, A. Atmanli, F.M. Vigil, Quaternary blends of diesel, biodiesel, higher alcohols and vegetable oil in a compression ignition engine, *Fuel* 212 (2018) 462–469.
- M.S. Peer, R. Kasimani, S. Rajamohan, P. Ramakrishnan, Experimental evaluation on oxidation stability of biodiesel/diesel blends with alcohol addition by rancimat instrument and FTIR spectroscopy, *J. Mech. Sci. Technol.* 31 (1) (2017) 455–463.
- A. Vrhovsek, O. Gereben, A. Jamnik, L. Pusztai, Hydrogen bonding and molecular aggregates in liquid methanol, ethanol and 1-propanol, *J. Phys. Chem. B* 115 (46) (2011) 13473–13488.
- W.A. Fouad, L. Wang, A. Haghmoradi, S.K. Gupta, W.G. Chapman, Understanding the thermodynamics of hydrogen bonding in alcohol-containing mixtures: self association, *J. Phys. Chem. B* 119 (44) (2015) 14086–14101.
- W. Wagner, A. Pru, The IAPWS formulation 1995 for the thermodynamic properties of ordinary water substance for general and scientific use, *J. Phys. Chem. Ref. Data* 31 (2002) 387–535.
- E.W. Lemmon, M.L. Huber, M. McLinden, Reference fluid, thermodynamic, transport properties. In: NIST Standard Reference Database 23, version 9.0; The National Institute of Standards, Technology: Gaithersburg, MD, 2010.
- F. Neese, The ORCA program system, *WIREs Comput. Mol. Sci.* 2 (2012) 73–78.
- C. Lee, W. Yang, R.G. Parr, Development of the Colle-Salvetti correlation-energy formula into a functional of the electron density, *Phys. Rev. B* 37 (1988) 785–789.
- A.D. Becke, Density-functional exchange-energy approximation with correct asymptotic behavior, *Phys. Rev. A* 38 (1988) 3098–3100.
- A.D. Becke, Density-functional thermochemistry. III. The role of exact exchange, *J. Chem. Phys.* 98 (1993) 5648–5652.
- S. Grimme, J. Antony, S. Ehrlich, H.A. Krieg, A consistent and accurate ab initio parametrization of density functional dispersion correction (DFT-D) for the 94 elements H-Pu, *J. Chem. Phys.* 132 (2010) 154104.
- S. Simon, M. Duran, J. Dannenberg, How does basis set superposition error change the potential surfaces for hydrogen-bonded dimers?, *J. Chem. Phys.* 105 (1996) 11024.
- R.F.W. Bader, *Atoms in Molecules: A Quantum Theory*, 1990 (Oxford).
- T. Lu, F. Chen, Multiwfn: A multifunctional wavefunction analyzer, *J. Comput. Chem.* 33 (2012) 580–592.
- A.P. Lyubartsev, A. Laaksonen, M. DynaMix – a scalable portable parallel MD simulation package for arbitrary molecular mixtures. *Comput. Phys. Commun.* 128 (2000) 565–589.

- [45] V. Zoete, M.A. Cuendet, A. Grosdidier, O. Michelin, SwissParam, a fast force field generation tool for small organic molecules, *J. Comput. Chem* 32 (2011) 2359–2368.
- [46] L. Martínez, R. Andrade, E.G. Birgin, J.M. Martínez, PACKMOL: a package for building initial configurations for molecular dynamics simulations, *J. Comput. Chem.* 30 (2009) 2157–2164.
- [47] M. Tuckerman, B.J. Berne, G.J. Martyna, Reversible multiple time scale molecular dynamics, *J. Chem. Phys.* 97 (1992) 1990–2001.
- [48] U.L. Essmann, M.L. Perera, T. Berkowitz, H. Darden, H. Lee, L.G. Pedersen, A smooth particle mesh Ewald method, *J. Chem. Phys.* 103 (1995) 8577–8593.
- [49] M. Brehm, B. Kirchner, TRAVIS - A free analyzer and visualizer for Monte Carlo and Molecular Dynamics trajectories, *J. Chem. Inf. Model.* 51 (2011) 2007–2023.
- [50] U. Koch, P.L. Popelier, Characterization of C-H-O Hydrogen Bonds on the Basis of the Charge Density, *J. Phys. Chem.* 99 (1995) 9747–9754.